

Fatigue crack growth in a coarse-grained iron–silicon alloy

S.S. Chakravarthula, Y. Qiao*

Department of Civil Engineering, University of Akron, Akron, OH 44325-3905, USA

Available online 18 July 2005

Abstract

The fatigue crack growth in a coarse-grained Fe-2 wt% Si alloy is investigated in considerable detail. At room temperature, the material is quasi-brittle and the failure mode is mixed cleavage. Under a mode-I cyclic loading, the crack can overcome the barrier effect of grain boundaries, which dominates the overall damage evolution. Associated with the geometrically necessary crack front branching, there are two possible break-through modes for a fatigue crack to propagate across a high-angle grain boundary.

© 2005 Elsevier Ltd. All rights reserved.

Keywords: Grain boundary; Fatigue crack growth; Fe–Si alloy

1. Introduction

Over many years, the fatigue crack behavior in polycrystalline materials has been an active research area. Under the cyclic loading, the growth of a stage-I crack is along the energetically favorable persistent slip bands (PSB) and is dominated by the crack-tip opening/sliding displacement [1–3]. If the crack size is much longer than the characteristic microstructure length, the irreversible crack-tip plastic deformation becomes important, which leads to the power-law growth rate [4]. Currently, most of the researches in this area are focused on intrinsically ductile materials such as copper and aluminum alloys, where the factor of grain boundary comes in by affecting the dislocation reactions or the microvoid formation [5,6].

In intrinsically brittle materials such as steels, on the other hand, the fatigue behavior is strongly dependent of temperature. When the temperature is higher than the brittle-to-ductile transition (BDT) temperature, T_{BD} , the material behavior resembles that of ductile materials [7]. When the temperature is much lower than T_{BD} , the failure mode is pure cleavage, and the conventional fatigue damage does not occur. As the temperature increases, but is still lower than T_{BD} , plastic deformation becomes increasingly pronounced and mixed-cleavage mode dominates [8–10].

Under this condition, the mechanisms and processes that govern the fatigue damage evolution can be quite different from that at the upper shelf of BDT region.

In this paper, we measure the fatigue crack growth rate in a Fe-2 wt% Si alloy at room temperature, and analyze the role of grain boundaries through fractography study. The results indicate that the boundaries offer additional resistance to crack growth due to the geometrically necessary crack front branching, which would not only affect the growth rate, but also, according to the two-parameter theory [11–13], have significant influences on the threshold value.

2. Experimental

2.1. Sample preparation

The material under investigation was a Fe-2 wt% Si alloy provided by Professor Ali S. Argon, which consisted of 1.98 wt% of Si, 0.56 wt% of Al, 0.16 wt% of Mn, 0.26 wt% of Cu, 0.13 wt% of Cr, 0.14 wt% of Ni, and 0.038 wt% of Mo [9]. The original material was in hot-rolled plate form. Before testing, a $40 \times 15 \times 5$ mm strip was cut from the plate, decarburized in hydrogen environment at 1200 °C for about 2.5 h, and then electron-beam welded into a 304 stainless steel carrier, as depicted in Fig. 1. After the decarburization process, no carbides could be found on the fracture surfaces through SEM. The Vickers hardness was 226 kg/mm² [9]. The grain size was in the range of 1–10 mm, making it possible to directly observe the crack

* Corresponding author. Tel.: +1 330 972 2426; fax: +1 330 972 6020.
E-mail address: yqiao@uakron.edu (Y. Qiao).

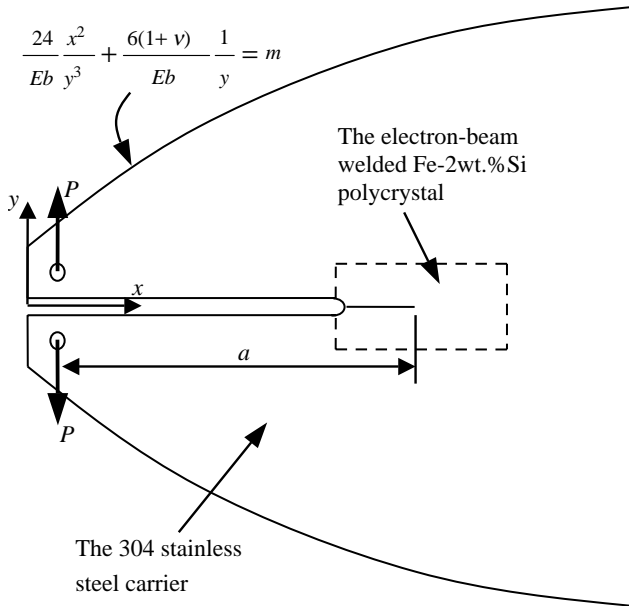


Fig. 1. A schematic diagram of the constant- K sample.

growth across individual grain boundaries. Due to the relatively small number of grains at the crack front, the fracture toughness of this material varied in a relatively broad range of 18–24 MPa $\sqrt{\text{m}}$.

The contour of the stainless steel carrier was determined by [14]

$$\frac{24}{Eb} \frac{x^2}{y^3} + \frac{6(1+\nu)}{Eb} \frac{1}{y} = m$$

where x and y are coordinates; E and ν are the Young's modulus and the Poisson's ratio, respectively; b is the sample thickness; and m is a geometry factor. In the current study, m was somewhat arbitrarily set to 4 N^{-1} , E was taken as 210 GPa, and ν was taken as 0.28. After the electron-beam welding, the specimen was ground to about 4 mm thick. Under the pin loading, the stress intensity factor at the crack tip can be calculated as $K = 2\sqrt{m/(1-\nu^2)}P/b$ [14], where P is the crack opening load per unit thickness. It can be seen that K is independent of the crack length, a . The gap between the two contoured arms served as the major part of the precrack. The precrack tip was produced by electrical discharge machining (EDM) using a 0.1 mm copper wire.

2.2. Fatigue experiment

The fatigue experiment was performed at room temperature. The sinusoidal cyclic loading was applied by a type 1365 hydraulic Instron machine. The frequency was 4 Hz. Due to the contoured sample geometry, the stress intensity at the crack tip remained constant during the experiment, regardless of the change in a . The maximum stress intensity factor, K_{max} , was 16.0 MPa $\sqrt{\text{m}}$, and the minimum stress intensity factor, K_{min} , was 0.

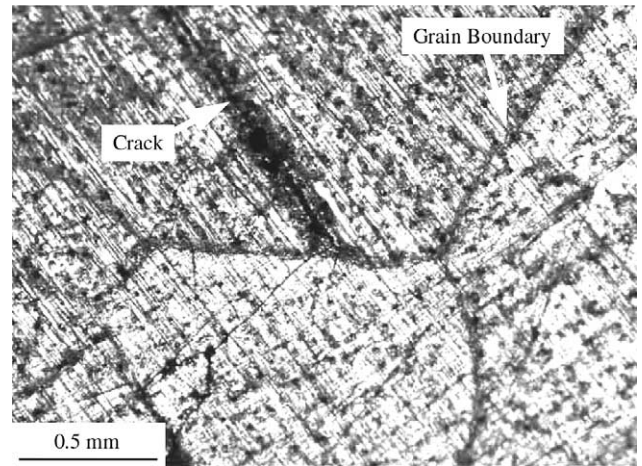


Fig. 2. The crack tip arrested by a high-angle grain boundary. The sample surface has been etched in 3% nital to show the grain boundaries.

During the fatigue test, photos of the near-tip field were taken periodically every 60 s using a Canon PS-G5 digital camera equipped by a set of Hoya lens. The shutter was controlled by a Zoombrowser-EX system. Thus, the crack length could be measured from the surface. The crack growth rate was calculated as $\Delta a/\Delta N$, where Δa is the increase in crack length after ΔN loading cycles. In order to show the grain boundaries clearly, the specimen was etched in 3% nital. Fig. 2 shows a fatigue crack with the tip arrested by a grain boundary, and Fig. 3 shows the crack growth rate, da/dN , as a function of the crack length. Note that, since in the constant- K sample, ΔK is independent of a , the variation in da/dN primarily reflects the effects of local crystallographic structure.

After the fatigue test, the sample was immersed in liquid nitrogen and broken apart cryogenically. The fracture surfaces were then observed through a JEOL JSM-5310 SEM. Fig. 4(a) shows the break-through mode of a fatigue crack across a high-angle grain boundary.

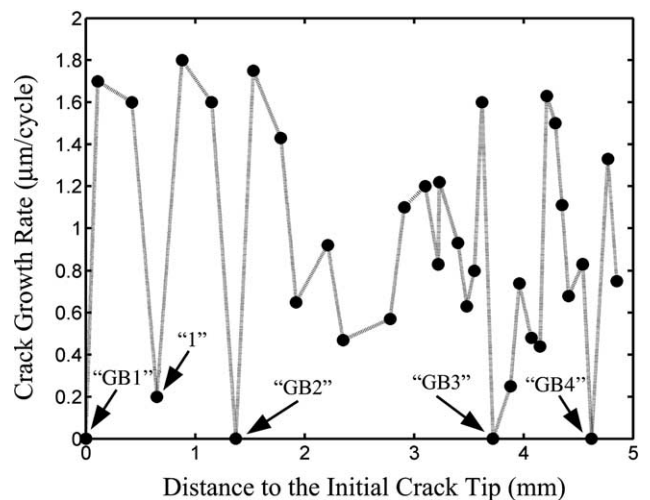


Fig. 3. The crack growth rate of the Fe-2 wt% Si sample. The points 'GB i ' ($i = 1, 2, 3, 4$) indicate grain boundaries.

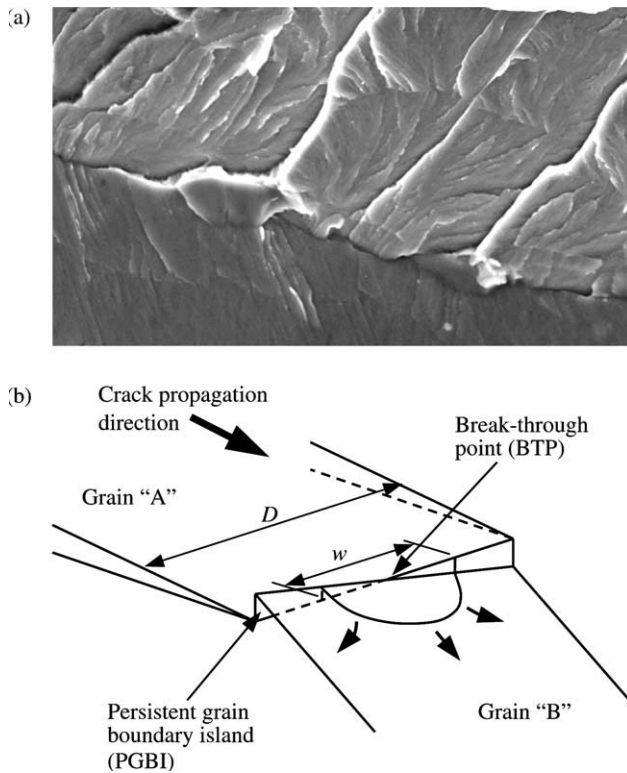


Fig. 4. The geometrically necessary crack front branching across a high-angle grain boundary: (a) the SEM fractography, where the crack propagation direction is from the bottom to the top; (b) a schematic diagram.

3. Results and discussion

As shown in Figs. 2 and 3, the crack growth rate was lowered significantly at the grain boundaries. Actually, at the sample surface no growth behavior could be detected when the crack tip was arrested at a grain boundary, and the points 'GBi' ($i = 1, 2, 3, 4$) in Fig. 3 were set to 0. After a certain loading cycles, often in the range of 10,000–50,000, the crack 'suddenly' broke through the grain boundary and transmitted into the next grain. Therefore, although the crack growth rate inside a grain was quite high, it took 0.44 million cycles for the fatigue crack to grow by about 8 mm.

Unlike that in purely ductile materials, the fatigue crack growth inside a grain of the Fe-2 wt% Si alloy does not demonstrate striations associated with the crack tip opening and closure. Instead, according to the fractography shown in Fig. 4(a), the crack growth is caused by stoppage and reinitiation of mixed-cleavage facets. This is in consistent with the observation of crack growth in a Fe-3 wt% Si alloy, in which, although the fracture appearance was cleavage-like, the shear of ligaments led to a high toughness [8]. Similar phenomena of ductile–brittle and brittle–ductile transition were also reported for other materials at near-BDT temperatures, e.g. Ref. [4].

From the fracture surfaces, it can be seen clearly that the break-through process is highly nonuniform. The crack front first 'penetrates' across the grain boundary at a number of break-through points (BTP) that distribute along the front quasi-periodically. The distance between the BTP, D , ranges from 1 to 20 μm . When the width of a BTP, w , reaches a certain value, with the separation the persistent grain boundary islands (PGBI), the grain boundary is overcome and the crack continues to advance in the adjacent grain (Fig. 4(b)).

It was observed occasionally from the sample surface that the crack growth rate could also be lowered by an order of magnitude inside a grain, e.g. at point '1' in Fig. 3. Fractography study revealed that such a low growth rate always occurred at the protruding part of the verge of propagating, with the rest of the front arrested by grain boundaries in the interior, which caused a decrease in local stress intensity [8,9]. Thus, again, it can be attributed to the grain boundary resistance.

4. Possible break-through modes across a high angle grain boundary

As the crack front gradually penetrates through a grain boundary, with the increasing of the penetration depth, a , the persistent grain boundary islands between the BTP are subjected to an increasingly large bridging force. While the fractography study provides little information of the details of the PGBI separation, according to the discussions of transgranular fracture in open literature [8,15,16], there are two possible modes.

4.1. Mode II fatigue damage evolution

The first possible mode of PGBI separation is the coplanar fatigue crack growth along the boundary, as depicted in Fig. 5(a). The PGBI act as reinforcements bridging across adjacent cracked grains, where the mode II fatigue crack growth can be triggered. When the length of the mode II intergranular crack reaches the critical value, c_{cr} , the height difference between the adjacent crack planes is reduced to h_{cr} , such that the grain boundary resistance can be overcome at the maximum stress intensity factor, K_{max} . With given initial height difference h_0 , the required force to overcome a grain boundary containing an intergranular crack is

$$F_0 = \frac{1}{2} k w h_{cr} = \frac{1}{2} k w h_0 (1 - 2\tilde{c}) \quad (1)$$

where k is the effective shear strength of the grain boundary, and $\tilde{c} = c_{cr}/h_0$. Integration with respect to the shear distance, δ , gives the fracture work

$$W_0 = \int_0^{\delta^*} F_0 d\delta \approx \frac{1}{2} k w h_0 (1 - 2\tilde{c}) \delta^* \quad (2)$$

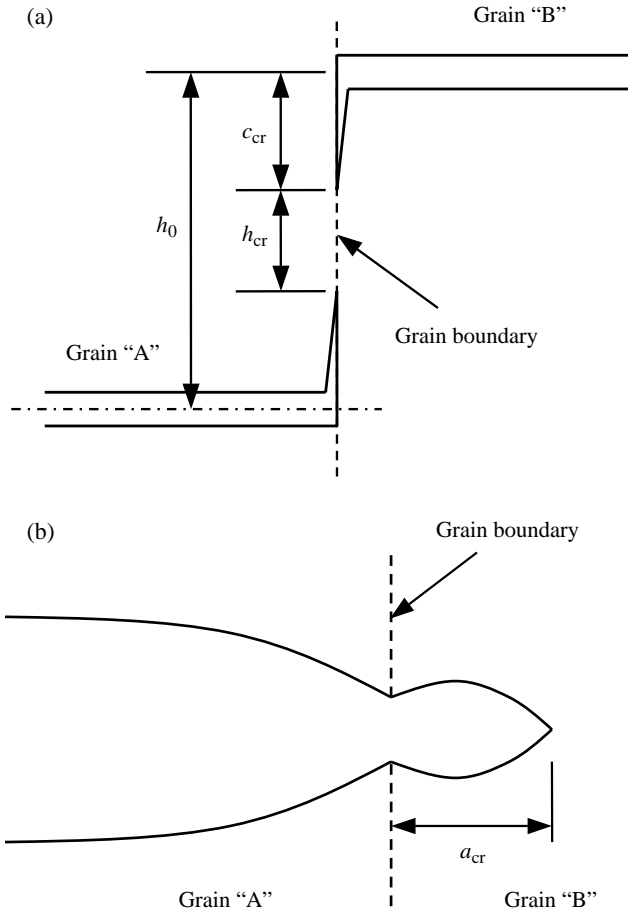


Fig. 5. Two possible modes for a crack to overcome a high-angle grain boundary: (a) coplanar fatigue crack growth along the grain boundary; (b) abrupt separation of the persistent grain boundary islands.

where δ^* is the maximum shear distance. In Eq. (2), the variation in F_0 is ignored. For the first-order approximation, the value of δ^* can be assessed as h_{cr} [15]. Hence, under the critical condition, we have

$$K_{max} = \sqrt{\frac{EG_{cr}}{1-\nu^2}} = \sqrt{\frac{Ekw}{2(1-\nu^2)} \tan \varphi \cdot (1-2\bar{c})} \quad (3)$$

where $G_{cr} = W_0/w^2$ is the critical fracture resistance and φ is the twist crystallographic misorientation. Note that h_0 is estimated as $w \cdot \tan \varphi$. Eq. (3) can be rewritten as

$$\frac{2c_{cr}}{h_0} = 1 - K_{max} \cot \varphi / \sqrt{\frac{Ekw}{2(1-\nu^2)}}, \quad (4)$$

which gives the required c_{cr} at which the grain boundary can be overcome under K_{max} . When $K_{max} \geq K_0 = \sqrt{Ekw/2(1-\nu^2)} \tan \varphi$, the value of $c_{cr} \leq 0$, indicating that the grain boundary cannot provide sufficient resistance to arrest the crack and will be sheared apart in the first cycle; that is, the fatigue does not occur. If we take E as 210 GPa; k as $\sigma_y/\sqrt{3}$, where the tensile strength σ_y can be assessed through $\sigma_y/E = 0.005$; w as 10 μm ; φ as 22.5°; and ν

as 0.28, the value of K_0 is about 24 $\text{MPa}\sqrt{\text{m}}$, which is quite reasonable. When $K_{max} < K_0$, the barrier effect of the grain boundary cannot be overcome through fracture, until the intergranular crack length reaches c_{cr} given by Eq. (4). For $K_{max} = 16 \text{ MPa}\sqrt{\text{m}}$ and $\varphi = 22.5^\circ$, $2c_{cr}/h_0$ is about 0.2. With constant φ and w , c_{cr} decreases as K_{max} increases, as it should.

4.2. Abrupt grain boundary separation

While the above analysis of the mode II fatigue crack growth in PGBI is self-compatible, there is no supporting evidence that can be found by the fractography study. No cyclic markings could be observed in any separated PGBI. This can be caused by the ‘smear’ effect during the final separation of fracture surfaces that smoothens all the features. However, another possible explanation is that the mode II crack initiation is difficult, especially at the clean boundaries [8]. Therefore, once a mode II crack is formed it can propagate rapidly, i.e. the PGBI are separated through an abrupt fracture process, as shown in Fig. 5(b).

This assumption can be analyzed in context of R -curve theory. Under the cyclic loading, the fatigue front penetrates across the grain boundary at the break-through points. As the penetration depth becomes larger and larger, more and more grain boundary areas are separated, leading to a lower rate of fracture work increment. As long as the increasing rate of the work is larger than that of the crack growth driving force, the crack growth is stable. Due to the limitation of the grain boundary geometry, the increasing rate of the work keeps decreasing [16]. As a result, there exists a critical penetration depth, a_{cr} , at which the crack growth becomes unstable. The critical condition can be stated as [16]

$$\frac{K_{max}}{K_{SC}} = \left[1 + 0.12k_0 \left(\frac{\sin^2 \varphi \cos^2 \varphi \cos \psi}{\sin \varphi + \cos \varphi} \right)^{1.05} \right] \times \sqrt{\frac{\sin \varphi + \cos \varphi}{\cos \psi}} \quad (5)$$

where K_{SC} is the fracture toughness of a single crystal, ψ is the tilt crystallographic misorientation, and $k_0 = [(a_0/w)^\beta (\alpha^3/8)(k/\mu)(kw/G_{SC})]^{1.05}$, with a_0 being the crack length, α and β the geometry factors of the penetrating front, μ the shear modulus, and G_{SC} the fracture resistance of a single crystal. Based on Eq. (5), the critical penetration depth, a_{cr} , can be determined as [16]

$$\frac{a_{cr}}{w} = \left[\frac{2(1-\nu^2)K_{max}^2}{E(a_0 + a_{cr})\beta k^*} \frac{1}{(\sin \varphi \cos \varphi)^2} \right]^{1/\beta-1} \quad (6)$$

where $k^* = \alpha^3 k^2 / 8\mu$. For the Fe–Si alloy, α is about 3.0, β is around 0.8, and $k/\mu \approx 0.005$ [16]. Thus, for $K_{max} = 16 \text{ MPa}\sqrt{\text{m}}$ and $\varphi = 22.5^\circ$, a_{cr}/w is nearly 0.15, which seems plausible.

A vital factor involved in both of the break-through modes is the distance between the BTP, w . On the one hand, as w decreases, less persistent grain boundary areas are sheared apart, and thus the grain boundary resistance is lowered. On the other hand, a smaller w leads to a more pronounced crack-trapping effect, which tends to raise the boundary barrier. According to Eqs. (4) and (6), both c_{cr} and a_{cr} increase with w , indicating that the latter effect is dominant. However, currently the mechanisms of the break-through point formation are still quite inadequately understood. In a fracture experiment of Fe-3 wt% Si alloy [8], it was found that w is somewhat independent of the crystallographic misorientations. For the fatigue crack growth, this assumption needs to be further examined.

Clearly, the above discussion is only a first-order approximation. The details of the front propagation of fatigue cracks, e.g. the accumulated crack-tip damages, the effects of mixed mode loadings, and the anisotropy, are not taken into consideration. Nevertheless, this analysis depicts the basic process of fatigue crack growth across a high-angle grain boundary, based on which detailed numerical simulation can be carried out.

5. Conclusion

The crack growth behavior in a coarse-grained Fe-2 wt% Si alloy is investigated through a fatigue experiment at room temperature. The grain boundaries offer important resistance to the crack growth, which dominates the overall damage evolution. When a crack front encounters a grain boundary, the front first penetrates across the grain boundary at a number of break-through points. The grain boundary is overcome when the persistent grain boundary islands are separated. The following conclusions are drawn:

- (1) At room temperature, the fatigue crack growth in the Fe-2 wt% Si alloy is quite jerky.
- (2) The growth rate inside grains is much higher than that at grain boundaries.
- (3) The crack front must be branched geometrically necessarily to overcome a high-angle grain boundary.
- (4) There are two possible modes of the separation of persistent grain boundary islands.

Acknowledgements

We are grateful to Dr M. Hoo-Fatt and Dr T.S. Trivatsan for the help with the experiment.

References

- [1] Navarro A, de los Rios ER. Short and long fatigue crack growth: a unified model. *Phil Mag* 1988;57:15–36.
- [2] Li CS, Orlecky LJ. Fiducial grid for measuring microdeformation ahead of fatigue crack tip near aluminum bicrystal interface. *Exp Mech* 1993;33:286–92.
- [3] Bennett VP, McDowell DL. Polycrystal orientation distribution effects on microslip in high cycle fatigue. *Int J Fatigue* 2003;25:27–39.
- [4] McClintock FA, Argon AS. Mechanical behavior of materials. CBLIS; 1993.
- [5] Li CS. Crystallographic fatigue crack growth in incompatible aluminum bicrystals: its dependence on secondary slip. *Metall Trans* 1992;23A:3293–301.
- [6] Ellyin F, Li CS. The role of cyclic plasticity in crystallographic crack growth retardation. *Mater Sci Res Int* 1995;1:137–43.
- [7] Hertzberg RW. Deformation and fracture mechanics of engineering materials. New York: Wiley; 1989.
- [8] Qiao Y, Argon AS. Cleavage cracking resistance of high angle grain boundaries in Fe-3wt.%Si alloy. *Mech Mater* 2003;35:313–31.
- [9] Qiao Y, Argon AS. Cleavage crack-growth-resistance of grain boundaries in polycrystalline Fe-2wt.%Si alloy: experiments and modeling. *Mech Mater* 2003;25:129–54.
- [10] Qiao Y, Argon AS. Brittle-to-ductile fracture transition in Fe-3wt.%Si single crystals by thermal crack arrest. *Mech Mater* 2003;35:903–12.
- [11] Sadananda K, Holtz RL, Vasudevan AK. Critical examination of fatigue thresholds. In: Soboyejo WO, Lewandowski JJ, Ritchie RO, editors. Mechanisms and mechanics of fracture: The John Knott Symposium. TMS; 2002. p. 259–262.
- [12] Sadananda K, Vasudevan AK. Analysis of high temperature fatigue crack growth behavior. *Int J Fatigue* 1997;19:S183–S9.
- [13] Sadananda K, Vasudevan AK. A unified framework for fatigue damage analysis. *Naval Res Rev* 1998;50:56–68.
- [14] Mostovoy S, Crosley PB, Ripling EJ. Use of crack-line-loaded specimens for measuring plane-strain fracture toughness. *J Mater* 1967;2:661–81.
- [15] McClintock FA. A three dimensional model for polycrystalline cleavage and problems in cleavage after extended plastic flow or cracking. In: Chan KS, editors. George R. Irwin Symposium on Cleavage fracture. TMS; 1997. p. 81–94.
- [16] Qiao Y. Modeling of resistance curve of high-angle grain boundary in Fe-3wt.%Si alloy. *Mater Sci Eng* 2003;A361:350–7.